



## City Research Online

### City, University of London Institutional Repository

---

**Citation:** Nemra, A. & Aouf, N. (2010). Robust INS/GPS Sensor Fusion for UAV Localization Using SDRE Nonlinear Filtering. IEEE Sensors Journal, 10(4), pp. 789-798. doi: 10.1109/JSEN.2009.2034730

This is the accepted version of the paper.

This version of the publication may differ from the final published version.

---

**Permanent repository link:** <https://openaccess.city.ac.uk/id/eprint/22086/>

**Link to published version:** <https://doi.org/10.1109/JSEN.2009.2034730>

**Copyright:** City Research Online aims to make research outputs of City, University of London available to a wider audience. Copyright and Moral Rights remain with the author(s) and/or copyright holders. URLs from City Research Online may be freely distributed and linked to.

**Reuse:** Copies of full items can be used for personal research or study, educational, or not-for-profit purposes without prior permission or charge. Provided that the authors, title and full bibliographic details are credited, a hyperlink and/or URL is given for the original metadata page and the content is not changed in any way.

---

---



# Robust INS/GPS Sensor Fusion for UAV Localization using SDRE Nonlinear Filtering

A. Nemra<sup>1</sup> and N. Aouf<sup>2</sup>

Department of Informatics and Sensors,  
Cranfield University, Shrivenham. SN6 8LA, United Kingdom

<sup>1</sup>[a.nemra@cranfield.ac.uk](mailto:a.nemra@cranfield.ac.uk), <sup>2</sup>[n.aouf@cranfield.ac.uk](mailto:n.aouf@cranfield.ac.uk)

## Abstract

The aim of this paper is to present a new INS/GPS sensor fusion scheme, based on State-Dependent Riccati Equation (SDRE) nonlinear filtering, for Unmanned Aerial Vehicle (UAV) localization problem. SDRE navigation filter is proposed as an alternative to Extended Kalman Filter (EKF), which has been largely used in the literature. Based on optimal control theory, SDRE filter solves issues linked with EKF filter such as linearization errors, which severely decrease UAV localization performances. Stability proof of SDRE nonlinear filter is also presented and validated on a 3D UAV flight scenario. Results obtained by SDRE navigation filter were compared to EKF navigation filter results. This comparison shows better UAV localization performance using SDRE filter. The suitability of the SDRE navigation filter over an Unscented Kalman navigation filter for highly nonlinear UAV flights is also demonstrated.

**Keywords:** UAV Localization, Sensor Data Fusion, SDRE Nonlinear Filter, SDRE Stability.

## 1. Introduction

Over the last few years, Unmanned Aerial Vehicles (UAVs) have attracted attention in a number of civilian and military applications. They are able to perform tasks in highly hostile environments, where access to humans is limited. For these autonomous aerial vehicles, precise navigation is crucial in order to achieve high performance flights. Several sensing systems are used in UAV navigation such as: inertial navigation systems (INS), global positioning systems (GPS), air-data dead reckoning systems, radio navigation systems, and Doppler heading reference systems.

INS is the most used navigation sensor providing UAV position, velocity and attitude. However, it has small bias errors, which are continuously increasing with time. Hence, additional aerial vehicle position information from an accurate navigation sensor, such as GPS system, is required. GPS sensor will help to estimate the INS bias errors using a navigation filter, which will then give improved UAV position.

Nowadays, fusing data from different sensors to improve performance of the overall sensing system becomes necessary in various applications. For aerial navigation, fusion of GPS measurements with INS measurements by means of filtering techniques is vital to deliver the level of localization precision required by UAV missions.

Currently, the most used technique to fuse navigation data is Kalman filter [1]. Although Kalman filter is capable of providing real time vehicle position updates, it is based on linear system models and it suffers from linearization when dealing with nonlinear models. In this case, an extended Kalman filter (EKF) is adopted [2], where by means of Taylor series expansion, the nonlinear system is linearized and approximated around each current state estimate. Linear Kalman filter is then applied to produce the next state estimate. When large deviations between the estimated state trajectory and the nominal trajectory exist, the nonlinear model is weakly approximated by Taylor series expansion around the conditional mean. This makes high order terms of Taylor series expansion necessary. However, in the EKF, these high order terms are neglected.

Other data fusion techniques based on probabilistic approaches were presented and used in the literature. One of these techniques is Particle Filter (PF) [3], [4]. The main drawback of this filter is its computational requirement, which makes it not very suitable for real time applications such as aerial navigation problem. Approaches based on Unscented Transform (UT) resulted in a technique called Unscented Kalman Filter (UKF) [5]. This technique preserves the linear update structure of Kalman filter. It uses only second order system moments, which may not be sufficient for some nonlinear systems. In addition, the number of sigma points, used in UKF, is small and may not represent adequately complicated distributions. Moreover, unscented transformation of the sigma-points is computationally heavy, which is not suitable and practical for real time aerial navigation applications.

In this paper, we investigate an alternative to EKF based data fusion technique for UAV localization problem. This alternative is based on INS and GPS data and uses a State-Dependent Riccati Equations (SDRE) non-linear filtering formulation. SDRE techniques are rapidly emerging as optimal non-linear control and filtering methods. Over the past several years, various SDRE based design approaches have been successfully applied to aerospace problems. SDRE based designs have been used in advanced guidance [6, 7], in output feedback nonlinear  $H_2$  autopilot [8], and in full information nonlinear  $H_\infty$  autopilot [9]. Before that, a parameter-dependent Riccati equation technique was used in a pitch-yaw autopilot design where the parameter, roll rate, was exogenously supplied by a roll autopilot [10]. In addition, SDRE based design approaches have been applied to the control design for a nonlinear benchmark problem [11, 12].

In [13], SDRE nonlinear regulation, SDRE nonlinear  $H_\infty$  and SDRE nonlinear  $H_2$  design methodologies were defined and the optimality, sub optimality, and stability properties of SDRE nonlinear controllers were discussed. In [14], the SDRE nonlinear filter formulation was introduced and used for a pendulum-tracking problem. From the cited references, we notice that SDRE formulation was used more for control design problems and only a little for filtering problems. Moreover, these filtering problems are often related to small order systems.

The SDRE nonlinear filter is adopted here to avoid system linearization issues linked with the classical Extended Kalman filtering. However, SDRE filter stability is still an open research problem. Only very few papers introduced results on SDRE system stability proofs. These proofs were achieved for low order closed loop SDRE controlled systems [15, 16].

Contributions of this paper are mainly the development and validation of an alternative optimal INS/GPS filtering scheme based on SDRE technique for aerial (UAV) navigation problem and the global stability analysis developed for this SDRE nonlinear filtering system. The SDRE nonlinear filtering approach proposed in this work will present new option to aeronautical engineers for precise and real time aerial navigation. As the increase of autonomy of unmanned aerial vehicle is our interest, the ideal extension of this work is to use the SDRE nonlinear filtering in the simultaneous localization and mapping (SLAM) problem where navigation precision is crucial and where the SDRE stability study could be looked at to provide more consistency to SLAM operations.

This paper is organized as follows: Section 2 presents the navigation sensors (INS and GPS) used in this aerial localization problem. Section 3 describes shortly the Extended Kalman Filter. A review of the SDRE nonlinear filter, in addition, to its stability proofs are presented in Section 4. In section 5, simulation results of the SDRE nonlinear filter for the UAV localization problem are given and compared with the KF and EKF and UKF results.

## 2. INS/GPS Navigation

### A. INS/GPS navigation

#### A.1. Inertial Navigation System (INS)

The localization problem of an airborne system is formulated using the navigation core-sensing device: Inertial Measurement Unit (IMU). This unit measures the airborne platform acceleration ( $ax, ay, az$ ) and its rotation rates ( $p, q, r$ ) with high update rates. These measurements are then processed and transformed, at the Inertial Navigation System (INS), to provide the airborne platform position ( $X, Y, Z$ ), velocity ( $U, V, W$ ), and attitude ( $\phi, \theta, \psi$ ), fig.1.

Let us present the INS with the following nonlinear model:

$$\begin{cases} \dot{x}(t) = f(x(t), u(t), t) \\ y(t) = h(x(t), u(t), t) \end{cases} \quad (1)$$

where  $x$  is the state vector. This latter includes the position, the velocity and Euler angles.  $u$  represents the IMU outputs (angle rates, and accelerations).

$$x = [X, Y, Z, U, V, W, \phi, \theta, \psi]^T \quad (2)$$

$$u = [p, q, r, ax, ay, az]^T \quad (3)$$

The navigation equations require the definition of at least two reference frames. One reference frame is for the body/inertial (vehicle) representation and the other reference frame is for the navigation frame representation. Then, system equations of motion can be given by simple integrations and frame transformations as presented below.

#### A.1.1 Equations of motion:

Euler angle rates  $\dot{\phi}, \dot{\theta}, \dot{\psi}$  can be calculated using the following equation:

$$\begin{bmatrix} \dot{\phi} \\ \dot{\theta} \\ \dot{\psi} \end{bmatrix} = \begin{bmatrix} 1 & \sin(\phi)\tan(\theta) & \cos(\phi)\tan(\theta) \\ 0 & \cos(\phi) & -\sin(\phi) \\ 0 & \sin(\phi)\sec(\theta) & \cos(\phi)\sec(\theta) \end{bmatrix} \begin{bmatrix} p \\ q \\ r \end{bmatrix} \quad (4)$$

Assuming that the IMU is installed at the vehicle centre of gravity, the true vehicle acceleration in the body frame is given by  $\dot{U}, \dot{V}, \dot{W}$  as:

$$\begin{bmatrix} \dot{U} \\ \dot{V} \\ \dot{W} \end{bmatrix} = \begin{bmatrix} ax + Vr - Wq + g \sin(\theta) \\ ay - Ur + Wp - g \cos(\theta) \sin(\phi) \\ az + Uq - Vp - g \cos(\theta) \cos(\phi) \end{bmatrix} \quad (5)$$

The resulting acceleration vector is integrated with respect to time to obtain the velocity of the vehicle in the body frame as:

$$\begin{bmatrix} U \\ V \\ W \end{bmatrix} = \int \begin{bmatrix} \dot{U} \\ \dot{V} \\ \dot{W} \end{bmatrix} dt \quad (6)$$

The velocity vector is then integrated to read the position of the vehicle in the body frame. If the velocity is transformed down to the navigation frame and is integrated, we obtain the position vector  $[X, Y, Z]^T$  in the navigation frame as:

$$\begin{bmatrix} X \\ Y \\ Z \end{bmatrix} = \int C^{T}_{bn}(\phi, \theta, \psi) \begin{bmatrix} U \\ V \\ W \end{bmatrix} dt \quad (7)$$

where  $C_{bn}$  is the Direct Cosine Transform matrix that rotates a vector from the body frame to the navigation frame:

$$C_{bn} = \begin{bmatrix} c(\theta)c(\psi) & c(\theta)s(\psi) & -s(\theta) \\ s(\theta)s(\phi)c(\psi) - s(\psi)c(\phi) & s(\psi)s(\theta)s(\phi) + c(\psi)c(\phi) & s(\phi)c(\theta) \\ s(\theta)c(\phi)c(\psi) + s(\psi)s(\phi) & s(\phi)s(\theta)c(\phi) - c(\psi)s(\theta) & c(\phi)c(\theta) \end{bmatrix} \quad (8)$$

The Nonlinear INS state model is given by (9) as follows:

$$f(x, u) = \begin{bmatrix} \begin{bmatrix} c(\theta)c(\psi) & c(\theta)s(\psi) & -s(\theta) \\ s(\theta)s(\phi)c(\psi) - s(\psi)c(\phi) & s(\psi)s(\theta)s(\phi) + c(\psi)c(\phi) & s(\phi)c(\theta) \\ s(\theta)c(\phi)c(\psi) + s(\psi)s(\phi) & s(\phi)s(\theta)c(\phi) - c(\psi)s(\theta) & c(\phi)c(\theta) \end{bmatrix}^T \begin{bmatrix} U \\ V \\ W \end{bmatrix} \\ \begin{bmatrix} ax + Vr - Wq + g s(\theta) \\ ay - Ur + Wp - g c(\theta)s(\phi) \\ az + Uq - Vp - g c(\theta)c(\phi) \end{bmatrix} \\ \begin{bmatrix} 1 & s(\phi)\tan(\theta) & c(\phi)\tan(\theta) \\ 0 & c(\phi) & -s(\phi) \\ 0 & s(\phi)\sec(\theta) & c(\phi)\sec(\theta) \end{bmatrix} \begin{bmatrix} p \\ q \\ r \end{bmatrix} \end{bmatrix} \quad (9)$$

The observation model, related to the UAV position, based on the INS system is given by:

$$h(x, u) = \begin{bmatrix} 1 & 0 & 0 & 0 & 0 & 0 & 0 & 0 & 0 \\ 0 & 1 & 0 & 0 & 0 & 0 & 0 & 0 & 0 \\ 0 & 0 & 1 & 0 & 0 & 0 & 0 & 0 & 0 \end{bmatrix} \quad (10)$$

The problem with the navigation solution given by INS, Fig.1, is that it drifts with time as in most other dead reckoning systems. The drift rate of the inertial position is typically a cubic function of time. Small errors in gyros will be accumulated in angle estimates (roll and pitch), which in turn misrepresent gravitational acceleration as the vehicle acceleration and results in quadratic velocity (and cubic position) errors. This makes the development of any inertial only based localization solution very unsuitable. Therefore, INS requires reliable and effective additional information to reduce these errors. The additional source, providing aerial vehicle position, used in this paper is GPS.

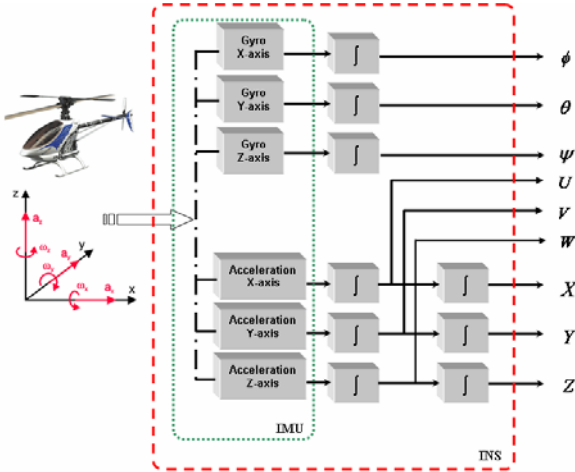


Fig.1 INS architecture

### A.1.2 INS errors

Most of INS errors are attributed to the inertial sensors (instrument errors). These are the residual errors exhibited by the installed gyros and accelerometers following calibration of the INS. The dominant error sources of INS system are shown in Table 1.

INS errors	Impact
Alignment errors	Roll, pitch and heading errors
Accelerometer bias or offset	A constant offset in the accelerometer output that changes randomly after each turn-on

Nonorthogonality of gyros and accelerometers	The accelerometer axes, gyro uncertainty and misalignment
Gyro drift or bias (due to temperature changes)	A constant gyro output without angular rate presence
Gyro scale factor error	Results in an angular rate error proportional to the sensed angular rate
Random noise	Random noise in measurements

Table 1: Sensor errors in INS

Due to mathematical integration, errors in the accelerations and angular rates lead to steadily growing errors in position and velocity of the aircraft. These are called navigation errors and there are nine of them - three position errors, three velocity errors, two attitude errors and one heading error. Gravity model can also cause INS errors, since variations, along the earth and with height, in the acceleration due to gravity are often not modelled accurately. If an unaided INS system is used, these errors grow with time and the INS position will largely drift from the true vehicle position as can be seen in Fig. 13 (red trajectory).

### A.2. Global Positioning System (GPS)

GPS uses a one-way ranging technique from GPS satellites, which are also broadcasting their estimated positions [17]. Signals from four satellites are used with the user generated replica signal and the measured relative phase. Using triangulation, the location of the receiver can be retrieved (Fig.2.a). Indeed, latitude, longitude, altitude and a correction to the user's clock are determined using four satellites in an appropriate geometry. The GPS receiver coupled with the computer receiver returns elevation angle and azimuth angle between the user and the satellite. These quantities are measured positive clockwise from the true north, geodetic latitude and longitude of the user. The GPS ranging signal is broadcasted at two frequencies: a primary signal at 1575.42 MHz (L1) and a secondary broadcast at 1227.6 MHz (L2). Civilians use L1 frequency, which has two modulations, viz. C/A or Clear Acquisition Code and P or Precise or Protected Code. C/A is unencrypted signal broadcast at a higher bandwidth and is available only on L1. P code is more precise because it is broadcasted at a higher bandwidth and is restricted for military use. The military operators can degrade the accuracy of the C/A code intentionally and this is known as Selective Availability. If we have a perfect clock in both the satellite and the receiver and if the signal is not affected by noise then precision in calculating the receiver position can be achieved (Fig.2.a). Otherwise an additional satellite is needed for time offset of the GPS receiver clock (Fig.2.b).

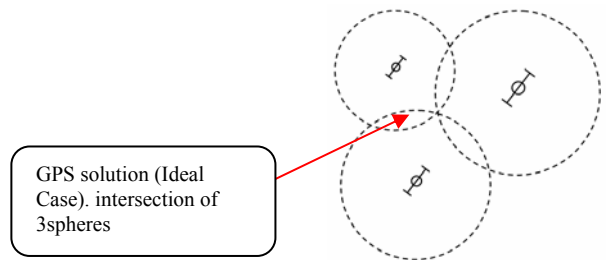


Fig.2.a Ideal case, 3 intersection spheres

In this paper, good precision of GPS signals is assumed. GPS ranging errors, [17], are assumed minimised using additional satellites, if necessary, to correct user's (UAV) clock. Thus, GPS signals are suitable to use in the sensor fusion process with the INS system by means of a navigation-filtering scheme, as illustrated in Fig.3.

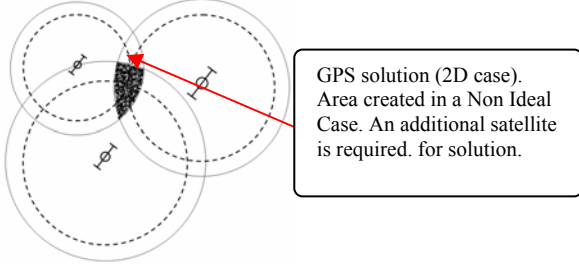


Fig.2.b Non ideal case, additional satellite is needed for time offset of the GPS receiver clock

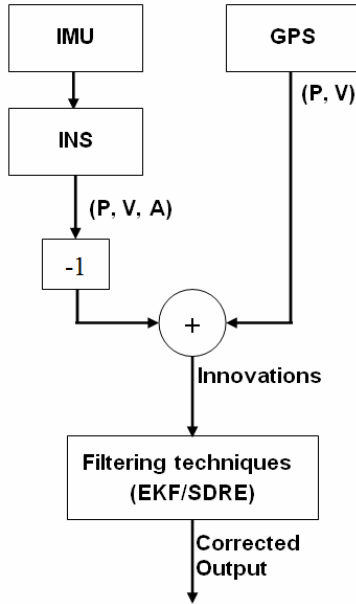


Fig.3 INS aided GPS sensor fusion

### 3. Extended Kalman Filter

Based on different estimation models, navigation filters are adopted as a sensor fusion scheme to obtain aerial vehicle states. One of these models, proposed in [1] and [2], is a linear model based on the error navigation model with assumptions on Euler angles (small Euler angles). In this case, a linear Kalman Filter is enough to use. However, those assumptions are generally not valid, which makes nonlinear filtering approaches, such as Extended Kalman Filter (EKF) as detailed below, required [2][18][19].

Our system, defined in (9) and (10), is converted to a non-linear discrete time state transition equation using the Zero-Order Hold (ZOH) function:

$$\begin{aligned} x_k &= f(x_{k-1}, u_k, w_k) \\ y_k &= h(x_k, v_k) \end{aligned} \quad (11)$$

$x_k$  is the state at time step  $k$ ,  $w_k$  is some additive noise,  $y_k$  is the observation made at time  $k$ ,  $v_k$  is some

additive observation noise. We assume that  $w_k$  and  $v_k$  are uncorrelated zero mean Gaussian with known covariance  $Q_k$  and  $R_k$ . The objective of the filtering technique is, then, to estimate  $x_k$  using available observation  $y_k$ .

The non-linear vehicle model and observation model maybe expanded around the filtered and predicted estimates of  $\hat{x}_k$  and  $\hat{x}_{k-1}$ .

$$\begin{aligned} x_k &= f(\hat{x}_{k-1/k-1}, u_k) + \Delta f_k(x) [x_k - \hat{x}_{k/k}] + \\ &\quad + \Delta_1 [x_k - \hat{x}_{k/k}] + [\Delta f_w(x) + \Delta_2 [x_k - \hat{x}_{k/k}]] w_k \end{aligned} \quad (12)$$

$$\begin{aligned} y_k &= h(\hat{x}_{k-1/k-1}, u_k) + \Delta h_k(x) [x_k - \hat{x}_{k/k-1}] + \\ &\quad + \Delta_3 [x_k - \hat{x}_{k/k-1}] + v_k \end{aligned} \quad (13)$$

where  $\Delta f_k(x)$  is the Jacobian of  $f$  evaluated at  $x_{k-1}$ ,  $\Delta f_w(x)$  the Jacobian of  $f/w_k$  evaluated at  $x_{k-1}$  and  $\Delta h_k(x)$  is the Jacobian of  $h$  evaluated at  $x_{k-1}$  and  $\Delta_{i=1,3}$  represents higher order terms of the Taylor series expansion.

The filter state error is defined as:

$$\tilde{x}_{k/k} = x_k - \hat{x}_{k/k} \quad (14)$$

The prediction error can be determined by subtracting the true state  $x_k$  from the prediction estimate as:

$$\tilde{x}_{k/k-1} = x_k - \hat{x}_{k/k-1} \quad (15)$$

Neglecting the high order terms of the Taylor series, the state and observation models can be rewritten as:

$$x_{k+1} = F_k x_k + \Gamma_k w_k \quad (16)$$

$$y_k = H_k x_k + v_k$$

where:  $F_k = \Delta f_k(\hat{x}_{k/k})$ ,  $\Gamma_k = \Delta f_w(\hat{x}_{k/k})$

EKF final form is written as a predictor-corrector scheme:

Predictor:

$$\hat{x}_{k+1/k} = f(\hat{x}_{k/k}, u_k, 0) \quad (17)$$

$$P_{k+1/k} = F_k P_{k/k} F_k^T + \Gamma_k Q_k \Gamma_k^T \quad (18)$$

Corrector:

$$\hat{x}_{kk} = \hat{x}_{kk-1} + K_k (y_k - H_k x_{k/k-1}) \quad (19)$$

$$K_k = P_{k/k-1} H_k^T (H_k P_{k/k-1} H_k^T + R_k)^{-1} \quad (20)$$

$$P_{k/k} = P_{k/k-1} - K_k H_k P_{k/k-1}$$

Unfortunately, when higher order terms of Taylor series are large, the nonlinear model in (11) is poorly approximated by (15), and EKF based estimation gives poor performances.

### 4. SDRE Nonlinear Filter

State-Dependent Riccati Equations (SDRE) techniques are used as control and filtering design methods based on State Dependent Coefficient (SDC) factorization [14]. In [20] and [21], infinite-horizon nonlinear regulator problem is shown as a generalization of time invariant infinite-horizon linear quadratic regulator problem where all system coefficient matrices are state-dependent. When these coefficient matrices are constant, the nonlinear regulator problem collapses with the linear regulator

problem and the SDRE control method collapses with the steady-state linear regulator. Filtering counterpart of the SDRE control algorithm is obtained by taking the dual system of the steady-state linear regulator and then allowing coefficient matrices of the dual system to be state-dependent [21]. The dual of the steady-state linear regulator is the steady-state continuous Kalman observer, which, in the absence of control, reduces to the steady-state continuous Kalman filter [21].

#### A. State Dependent Coefficient (SDC) Form:

Consider the nonlinear system:

$$\begin{aligned}\dot{\hat{x}} &= f(x, u) + \Gamma w \\ y &= h(x, u) + v\end{aligned}\quad (21)$$

$w$  and  $v$  are white noises with covariance matrices  $Q$  and  $R$ , respectively.

There are an infinite number of ways to transform this nonlinear system into an SDC form as:

$$\begin{aligned}\dot{\hat{x}} &= F(x, u)x + \Gamma w \\ y &= H(x, u)x + v\end{aligned}\quad (22)$$

where:  $f(x, u) = F(x, u)x$   $h(x, u) = H(x, u)x$

We note that the INS estimation model in (9) and (10) falls, by some equation manipulations, into an SDC form. This makes the SDRE filtering a very appealing technique to use for this sensor fusion based UAV localization problem.

#### B. SDRE Filter Equations:

SDRE filter uses system the SDC form and is given in [15] by:

$$\dot{\hat{x}} = F(\hat{x}, u)\hat{x} + K_f(\hat{x})[y(x) - H(\hat{x}, u)\hat{x}] \quad (23)$$

where

$$K_f(\hat{x}) = PH^T(\hat{x}, u)R^{-1} \quad (24)$$

and  $P$  is the positive definite solution of the algebraic Riccati equation:

$$F(\hat{x}, u)P + PF^T(\hat{x}, u) - PH^T(\hat{x}, u)R^{-1}H(\hat{x}, u)P + \Gamma Q\Gamma^T = 0 \quad (25)$$

Properties of SDRE techniques and their proofs are presented in [20] and [13] respectively. Nonlinear functions  $f(x, u)$  and  $h(x, u)$ , in (21), are considered as  $k$ -continuously derivable (i.e. belonging to  $C^k, k \geq 1$ ). In SDC parameterization,  $F(x, u)$  and  $H(x)$  are assumed to be smooth (i.e.  $C^k, k \geq 1$ ). This assumption is valid in our navigation problem since our SDC state parameters are reasonably slowly varying.

#### C. SDRE Stability:

Global stability of the SDRE nonlinear filter, as opposed to local stability of linear systems, is more difficult to demonstrate since getting stable eigenvalues of the discrete SDRE system at each sampling time does not guarantee global asymptotic stability. To the best of our knowledge, no formal stability proofs of the SDRE nonlinear filter were proposed in the literature. In the following, a method based on Lyapunov approach is

developed to provide, with all necessary conditions, the stability region of the SDRE nonlinear filter.

From equation (23), (24), we can write:

$$\dot{\hat{x}} = F(\hat{x}, u)\hat{x} + PH^T(\hat{x}, u)R^{-1}[y(x) - H(\hat{x}, u)\hat{x}] \quad (26)$$

$$\dot{\hat{x}} = (F(\hat{x}, u) - PH^T(\hat{x}, u)R^{-1}H(\hat{x}, u))\hat{x} + PH^T(\hat{x}, u)R^{-1}y(x) \quad (27)$$

By proposing a definite positive Lyapunov function  $V(\hat{x}) = \hat{x}^T P^{-1} \hat{x} > 0$ , the SDRE filter stability is guaranteed iff  $\dot{V}(\hat{x}) < 0$ , [22].

Using this Lyapunov function we get:  $\dot{V}(\hat{x}) = \dot{\hat{x}}^T P^{-1} \hat{x} + \hat{x}^T P^{-1} \dot{\hat{x}}$ . As  $\dot{P}^{-1} = 0$  (steady-state problem), then:

$$\dot{V}(\hat{x}) = 2\dot{\hat{x}}^T P^{-1} \hat{x} \quad (28)$$

Replacing (27) in (28), we obtain:

$$\dot{V}(\hat{x}) = 2\left[\dot{\hat{x}}^T F^T(\hat{x}, u)P^{-1}\hat{x} + \hat{x}^T H^T(\hat{x}, u)R^{-1}(y(x) - H(\hat{x}, u)\hat{x})\right] \quad (29)$$

Thus,  $\dot{V}(\hat{x}) < 0 \Leftrightarrow \hat{x}^T F^T(\hat{x}, u)P^{-1}\hat{x} < 0$  and

$$\hat{x}^T H^T(\hat{x}, u)R^{-1}[y(x) - H(\hat{x}, u)\hat{x}] < 0$$

Let us start by proving, under which conditions, the first term is defined negative.

$$1) \hat{x}^T F^T(\hat{x}, u)P^{-1}\hat{x} < 0 \quad (30)$$

Proof

This inequality is equivalent to have  $F(\hat{x}, u)P^{-1}$  as definite negative.  $P^{-1} > 0$  and  $F(\hat{x}, u)$  is the SDC form of  $f(x, u)$  and as mentioned earlier in the paper, SDC forms of a nonlinear function  $f$  are not unique. In the following, we propose to derive  $F_1(\hat{x}, u)$  and  $F_2(\hat{x}, u)$  as two SDC forms of  $f$ .

Then,  $F(\hat{x}, u, \alpha) = \alpha F_1(\hat{x}, u) + (1 - \alpha)F_2(\hat{x}, u)$ ,  $\alpha \in \mathfrak{R}$  is also an SDC form of  $f$  since

$$\begin{aligned}[\alpha F_1(\hat{x}, u) + (1 - \alpha)F_2(\hat{x}, u)\hat{x}] &= \alpha F_1(\hat{x}, u)\hat{x} + (1 - \alpha)F_2(\hat{x}, u)\hat{x} \\ &= \alpha f(\hat{x}, u) + (1 - \alpha)f(\hat{x}, u) = f(\hat{x}, u)\end{aligned}$$

$F(\hat{x}, u, \alpha)$  represents an infinite SDC parameterization family.  $\alpha$  is proposed as an extra parameter that can be used to build a suitable SDC from an infinite SDC form candidates  $F(\hat{x}, u, \alpha)$ . Using the SDC parameterization form  $F(\hat{x}, u, \alpha)$  in (30), the parameter  $\alpha$  should be chosen to comply with the first three statements, following, to achieve (30):

$$\begin{aligned}if F_1(\hat{x}, u) < 0 \text{ and } F_2(\hat{x}, u) < 0 \\ then if 0 < \alpha < 1 \Rightarrow F(\hat{x}, u) < 0 \\ if F_1(\hat{x}, u) < 0 \text{ and } F_2(\hat{x}, u) > 0 \\ then if \alpha > 1 \Rightarrow F(\hat{x}, u) < 0 \\ if F_1(\hat{x}, u) > 0 \text{ and } F_2(\hat{x}, u) < 0 \\ then if \alpha < 0 \Rightarrow F(\hat{x}, u) < 0 \\ if F_1(\hat{x}, u) > 0 \text{ and } F_2(\hat{x}, u) > 0 \\ then \forall \alpha \in \mathfrak{R} \Rightarrow F(\hat{x}, u) > 0\end{aligned}$$

Thus, a good choice of  $\alpha$  with two possible SDC forms  $F_1(\hat{x}, u)$  and  $F_2(\hat{x}, u)$  assures (30) to be definite negative. Worth to mention that for a more general case of  $k+1$  distinct SDC parameterizations, the dimension of  $\alpha$  will be of order  $k$  and  $F(\hat{x}, u, \alpha)$  will have the following form:

$$F(x, u, \alpha) = (1 - \alpha_k) F_{k+1}(x, u) + \sum_{i=1}^k \left( \prod_{j=1}^i \alpha_j \right) (1 - \alpha_{i-1}) F_i(x, u) \quad (31)$$

Let us examine, now, the second term, in (29), and see, under which conditions, its definite negative property holds:

$$2) \hat{x}^T H^T(\hat{x}) R^{-1} [y(x) - H(\hat{x}) \hat{x}] < 0 \quad (32)$$

The covariance matrix  $R$  is assumed diagonal  $R = \text{diag}(\sigma^2 x, \sigma^2 y, \sigma^2 z)$ . Since system observation is the GPS signal  $y(x) = [x_{gps} \ y_{gps} \ z_{gps}]^T$ , which is used by the observation matrix in (10), the inequality (32) becomes:

$$\frac{1}{\sigma^2 x} \hat{x}(x_{gps} - \hat{x}) + \frac{1}{\sigma^2 y} \hat{y}(y_{gps} - \hat{y}) + \frac{1}{\sigma^2 z} \hat{z}(z_{gps} - \hat{z}) < 0$$

$$\frac{(\hat{x} - \frac{x_{gps}}{2})^2}{\sigma^2 x} + \frac{(\hat{y} - \frac{y_{gps}}{2})^2}{\sigma^2 y} + \frac{(\hat{z} - \frac{z_{gps}}{2})^2}{\sigma^2 z} > D \quad (33)$$

where

$$D = \left( \frac{x_{gps}}{2\sigma x} \right)^2 + \left( \frac{y_{gps}}{2\sigma y} \right)^2 + \left( \frac{z_{gps}}{2\sigma z} \right)^2 \quad (34)$$

This inequality defines the outside region of an ellipsoid centred at  $C = \left[ \frac{x_{gps}}{2} \ \frac{y_{gps}}{2} \ \frac{z_{gps}}{2} \right]^T$  and with semi-majors:  $r_x = \sigma x \sqrt{D}$ ,  $r_y = \sigma y \sqrt{D}$ ,  $r_z = \sigma z \sqrt{D}$ .

If  $\alpha$  is chosen properly assuring the definite negative property of the first term of  $\dot{V}$  in (30), we can claim that the region, specified by (33) defines the stability region of our SDRE nonlinear filter, as shown in Fig.4.

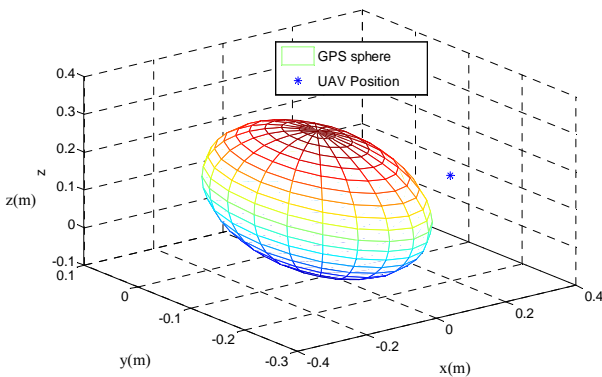


Fig.4 Ellipsoid region of stability (outside the ellipsoid)

Let us now evaluate the stability of the SDRE nonlinear filter if the states of the navigation system get inside the ellipse, which implies that  $\dot{V} \geq 0$ . In this case and from (28), we get:

$$\dot{\hat{x}}^T P^{-1} \hat{x} = \hat{x}^T P^{-1} \dot{\hat{x}} \geq 0 \quad (35)$$

Then, for small values of  $\Delta t$ , we can use numerical derivative to obtain:

$$\hat{x}_k^T P^{-1} \left( \frac{\hat{x}_{k+1} - \hat{x}_k}{\Delta t} \right) \geq 0 \quad (36)$$

$$\hat{x}_k^T P^{-1} (\hat{x}_{k+1} - \hat{x}_k) \geq 0 \quad (37)$$

$$\hat{x}_k^T P^{-1} \hat{x}_{k+1} \geq \hat{x}_k^T P^{-1} \hat{x}_k \quad (38)$$

To well understand the meaning and the use of these equations, let us represent the inequality (38) by vectors,  $\vec{i}$  of coordinates  $\hat{x}_k^T P^{-1}$ ,  $\vec{e}_k$  of coordinates  $\hat{x}_k$  and  $\vec{e}_{k+1}$  of coordinates  $\hat{x}_{k+1}$ . Then equation (38) becomes:

$$\vec{i} \cdot \vec{e}_{k+1} \geq \vec{i} \cdot \vec{e}_k \quad (39)$$

On the other hand and because  $P^{-1} > 0$  and  $\hat{x}_k^T P^{-1} \hat{x}_k > 0$  then:

$$\vec{i} \cdot \vec{e}_k > 0 \quad (40)$$

This later inequality signifies that  $\cos(\vec{i}, \vec{e}_k) > 0$ , which means that the angle between  $\vec{i}$  and  $\vec{e}_k$ , is stuck between  $]-\pi/2, \pi/2[$  as shown in Fig.5. Thus, we can state that the vector  $\vec{i}$  diverges from the origin and tries to get out of the ellipse.

Combining this result with the inequality (39), we can conclude that the projection of  $\vec{e}_{k+1}$  on  $\vec{i}$  is larger than the projection of  $\vec{e}_k$  on  $\vec{i}$ , which implies that the vector  $\vec{e}_{k+1}$  diverges from the origin more than  $\vec{e}_k$ . We obtain, then, the following final result:

$\forall \vec{e}_k(\hat{x}_k)$ , such that  $\|\vec{e}_k\| < D$ , then  $\vec{e}_{k+1}(\hat{x}_{k+1})$  attempts to diverge from the origin, i.e. tries to return back (attraction) to the stability region.

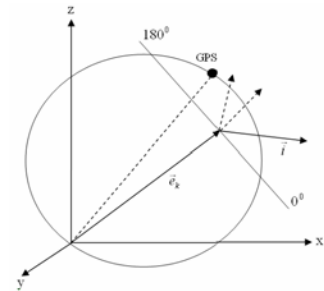


Fig.5 Stability inside the ellipse

This result shows that, whenever the SDRE filter provides state estimates that bring the system at the frontiers of the inside ellipsoid region, which implies  $\dot{V} \geq 0$ , and thus no guarantees of the global filter stability, the SDRE nonlinear filter will bring back the system to the region of stability shown on Fig.4. This way, we showed that the inequality in (32) is globally verified and for the SDRE nonlinear filter stability, a good choice of the parameter  $\alpha$  is sufficient to assure it. In Fig.6, we illustrate graphically the main steps of the SDRE filter stability proof presented above.



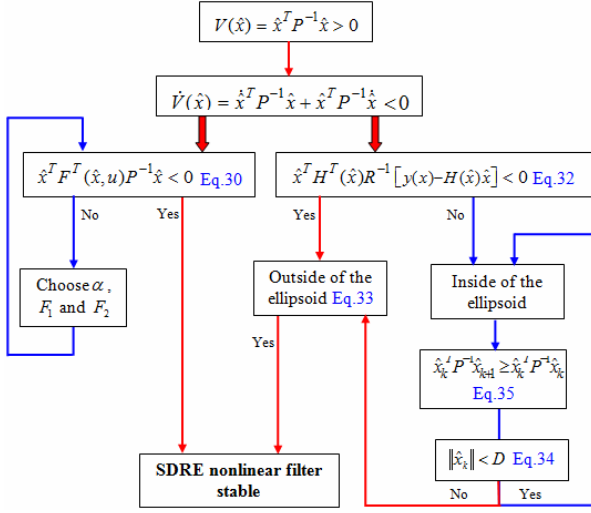


Fig.6 Proof of stability scheme

## 5. Simulation Results

We present our simulation results to validate the proposed nonlinear SDRE filter for the autonomous airborne navigation problem. The results of our approach are compared with other navigation filtering approaches. Following are the simulations conducted: firstly, we apply Kalman Filter to an INS error model, which is linear under the assumption that Euler angles are small. Then, an Extended Kalman Filter (EKF) is applied to a nonlinear INS model. Last simulations are based on the proposed SDRE nonlinear filter. Comparison of SDRE with UKF navigation results is also highlighted. The sampling rates used for each sensor and filter, in this study, are as follows:

$$f_{INS} = 100\text{Hz}, f_{SDRE} = 10\text{Hz}, f_{EKF} = 10\text{Hz}, f_{GPS} = 1\text{Hz}.$$

Simulation results shown in Fig.7, Fig.8, and Fig.9 represent the estimated UAV position obtained by KF, EKF and SDRE filters respectively, for the 3D trajectory given by Fig.13.

KF estimation is adequate only for small airborne angular rates. However, if this assumption does not hold, and that is generally the case, then the estimation performance is poor as presented in Fig.7.

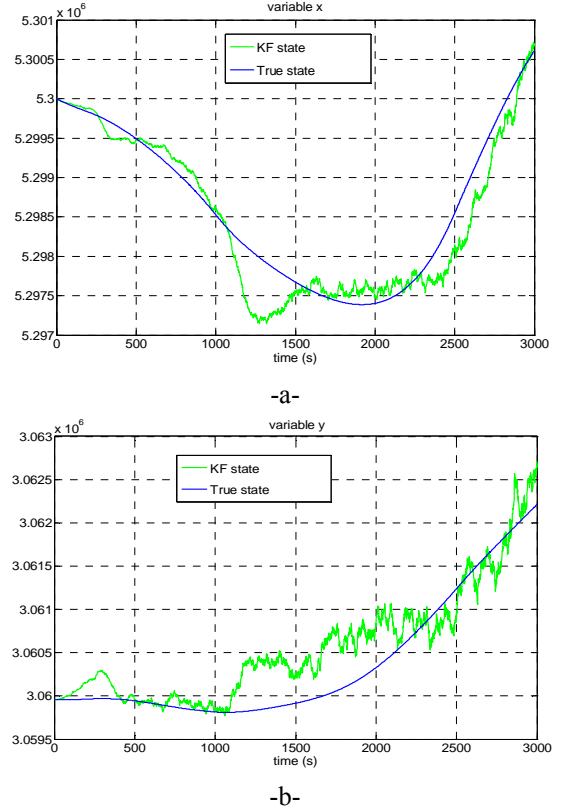
From Fig.8 (a, b), EKF is shown to perform much better than KF for a smooth trajectory. Unfortunately, EKF performance degrades when facing strong nonlinearities. In this case, the Jacobian matrix is ill conditioned, which causes undesirable bumps in the estimated coordinates as shown in Fig.8 (c) (z variable presents nonlinearities).

Fig.9 presents the airborne position estimated by SDRE nonlinear filter, which is based on two appropriate SDC forms  $F_1$ ,  $F_2$  and a suitable value of  $\alpha = 0.5$ . It is clear that the estimation results are improved with SDRE filter in comparison to KF and EKF filters. We can observe that for strong nonlinearities, the SDRE estimation error increases slightly but it is still within the tolerance for the localization problem in comparison to KF and EKF estimation methods.

Table.2 shows, for a number of simulation tests, a comparison in terms of standard deviation between the true state and the filter (KF, EKF, UKF and SDRE) outputs. A better precision of UAV position in the navigation frame is obtained by the SDRE filter with standard deviations  $\sigma_x = 4.0513\text{m}$   $\sigma_y = 1.2580\text{m}$

$\sigma_z = 3.0705\text{m}$  after 50 min of navigation. Similar to results in few recent research on vehicle navigation [23, 24], Table 2 shows that EKF could lead in few cases to similar results than UKF navigation results. However, UKF is very much more precise than EKF when UAV trajectory is highly nonlinear as in the z-channel of the proposed simulation example.

Table.2 and Fig.10 present a comparison between Unscented Kalman Filter (UKF) and the non-linear SDRE filter. As can be seen from Fig.10, both UKF and SDRE provide good and similar estimations of the UAV z position. Although SDRE results showed a minor improvement over UKF results in Table.2, this similarity in performance between SDRE and UKF generally holds. However, UKF filter as expected and as mentioned in the introduction of this paper is computationally heavier (Table.3) because of the unscented transformation applied on each sigma-point. From Fig.10 and Fig.13, we can definitely notice that SDRE estimated trajectory is smoother than the UKF estimated trajectory. This is expected as we are dealing with a highly nonlinear navigation system and a sharp UAV trajectory.



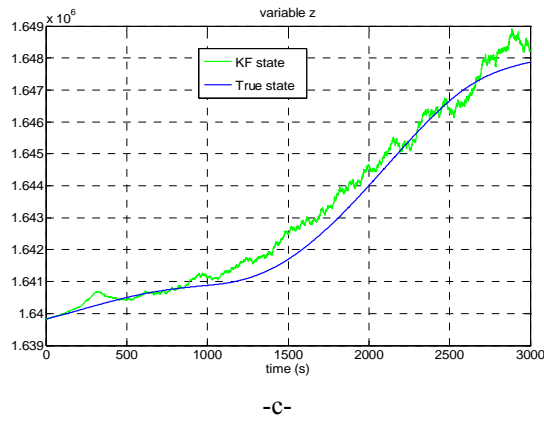


Fig.7 Estimated position of the airborne, with Kalman Filter (Linear error model)

	$\sigma_x(m)$	$\sigma_y(m)$	$\sigma_z(m)$
KF	59.0247	23.8104	49.2331
EKF	3.4187	2.9710	7.8191
UKF	3.1234	3.1995	3.5681
SDRE	4.0513	1.2580	3.0705

Table.2 Comparison of the standard deviation between KF (linear error model), EKF (linearized model), UKF (Non-linear system) and SDRE (Non-linear system).

	EKF	UKF	SDRE
Required time for 100 iterations (s)	0.5670	8.4500	1.5000

Table.3 Comparison of the computation time between EKF, UKF and SDRE

In the second part of the simulation, we validate the theoretical stability results obtained in section 4.C. These results define the exterior of an ellipsoid, (Fig.4), as the safe and stable flight navigation region for the UAV. As shown in Fig.11, whenever the UAV is inside or attracted to the GPS ellipsoid (inside the sphere), it is pushed back to remain outside of the ellipsoid to guarantee the stability of the SDRE nonlinear filter. Fig.12, presents SDRE (blue) and GPS (red) sphere radiuses for the entire simulation time. The convergence of the two radiuses validates the results shown in Fig.11. Finally, GPS, INS, true and estimated (EKF, UKF and SDRE) 3D UAV trajectories are shown in Fig.13.

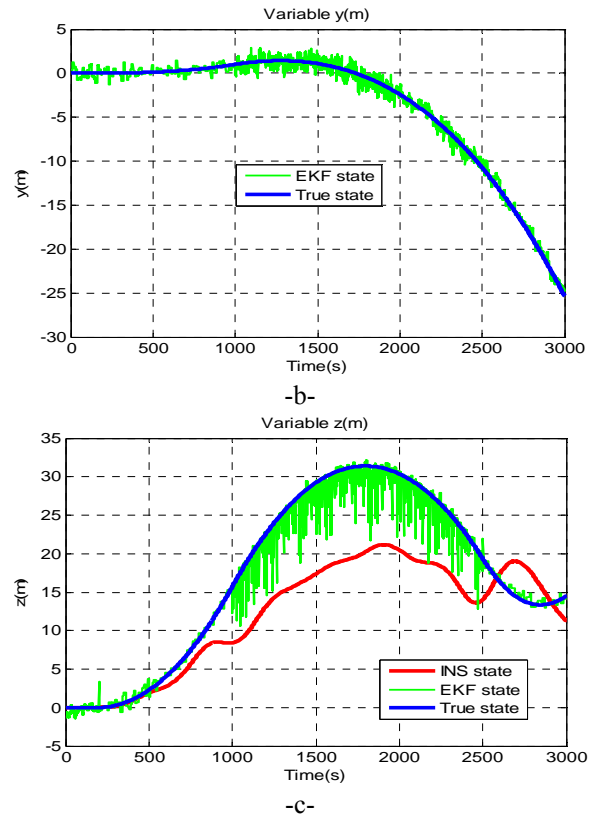
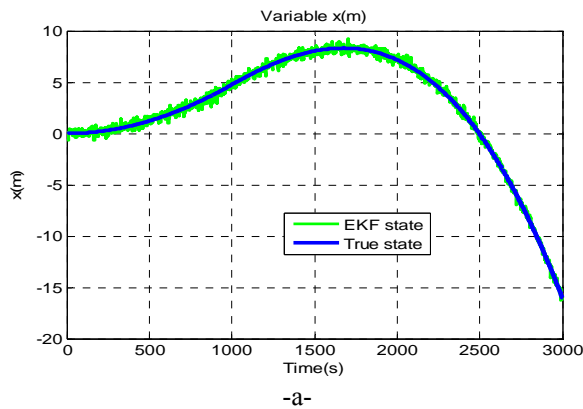
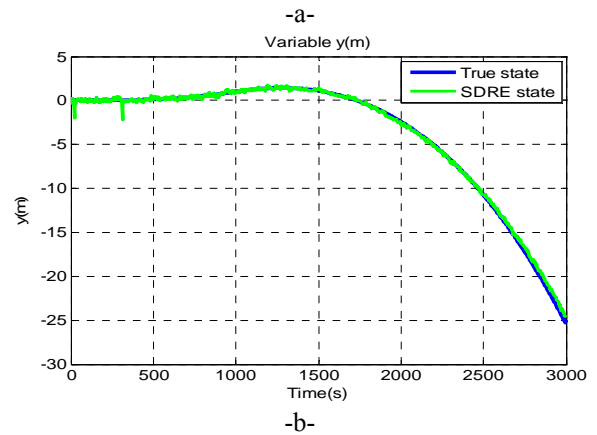
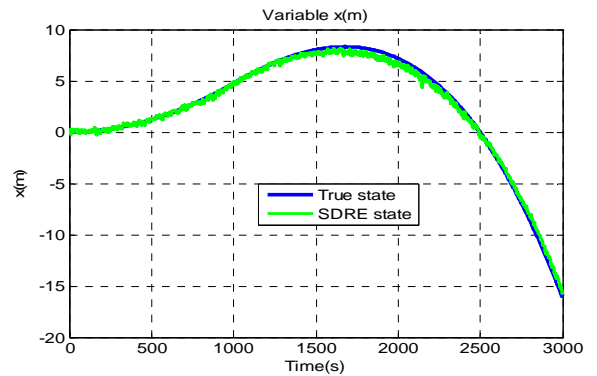


Fig.8 Estimated position of the airborne, with Extended Kalman Filter (Linearized model)



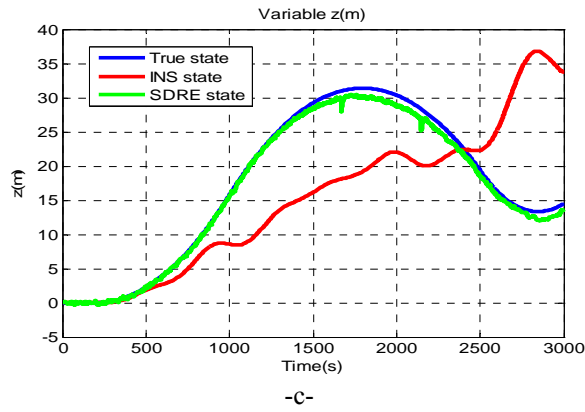


Fig.9 Estimated position of the airborne, with the SDRE Nonlinear filter (Non-linear model)

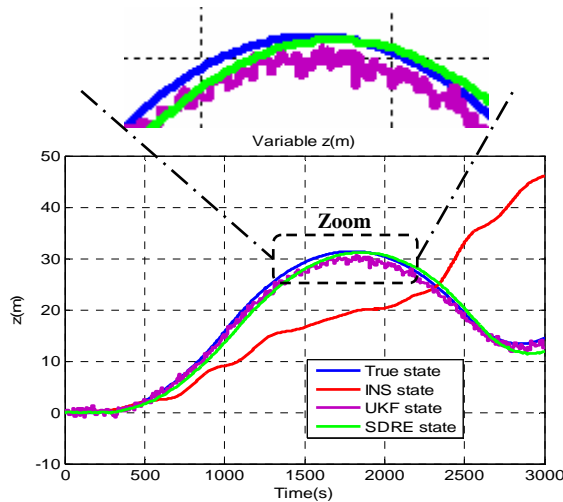


Fig.10 Estimated of the airborne z position, comparison between UKF and SDRE.

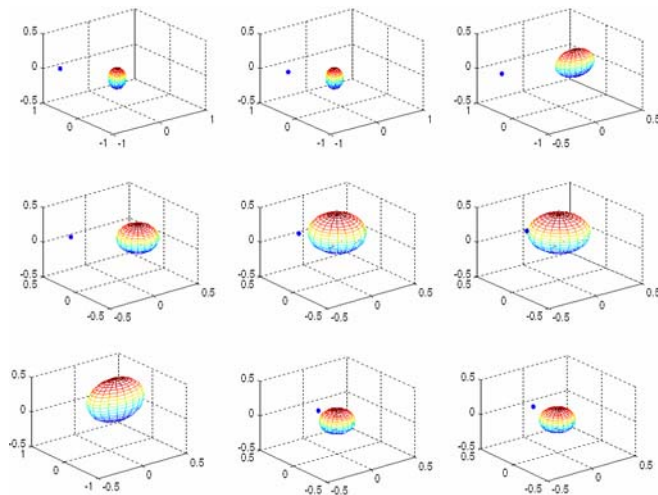


Fig.11 UAV position and Stability region in the navigation frame

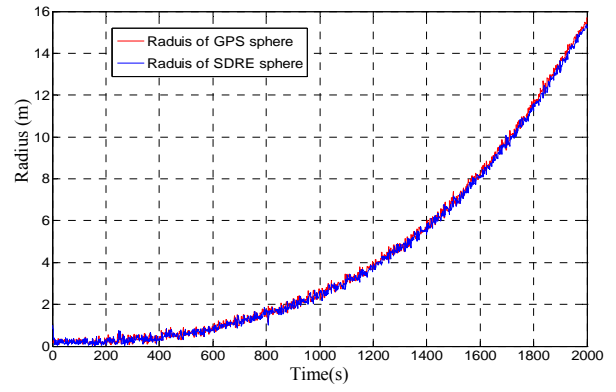


Fig.12 GPS and SDRE Sphere radius during the time of simulation

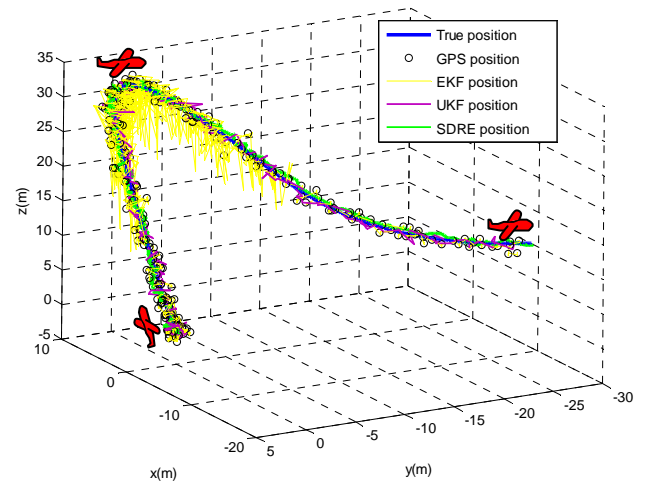


Fig.13 UAV trajectory, and estimated positions

## Conclusion

In this paper, we proposed a State-Dependent Riccati Equation (SDRE) nonlinear filter to estimate the location of an unmanned aerial vehicle (UAV), using INS/GPS data. The proposed method solves issues related to linearization, which poses problem for the classical filtering techniques like the Extended Kalman Filter (EKF). We have compared the performances of our filter with other filters (KF, EKF) performances. Good results were obtained with the SDRE nonlinear filter particularly in the case of strong nonlinearities. Formal proofs of the SDRE nonlinear navigation filter stability were proposed and a stability attractive region was determined. In our future work we will use the SDRE nonlinear filter to solve the Simultaneous localization and mapping problem of unmanned aerial vehicles with real time experiments.

## References

- [1] Vikas Kumar N "Integration of Inertial Navigation System and Global Positioning System Using Kalman Filtering" Aerospace Engineering, Department of Aerospace Engineering Indian Institute of Technology, BOMBAY Mumbai July 2004.

- [2] Sven Ronnback "Development of an INS/GPS navigation loop for an UAV", Master's Thesis 2000, ISSN: 1402-1617. ISRN: LTU-EX00/081-SE, Lulea Tekniska Universitet.
- [3] M. K. Pitt and N. Shephard, "Filtering via simulation: auxiliary particle filters" J. Amer. Statist. Assoc., vol. 94, no. 446, pp. 590–599, 1999.
- [4] S. Arulampalam, S. Maskell, N. Gordon, and T. Clapp, "A tutorial on particle filter for on-line nonlinear/nongaussian bayesian tracking,," IEEE Trans. Signal Process., vol. 50, no. 2, pp. 174–188, 2002.
- [5] S. Julier and J. Uhlmann, "A new extension of the Kalman filter to nonlinear systems" in Int Symp, Aerospace/Defense Sensing, Simul and Controls, Orlando, Proceedings Vol. 3068, pp.182-193, FL, 1997.
- [6] J. R. Cloutier "Adaptive matched augmented proportional navigation". Presented at the AIAA Missile Sciences Conference, November 1994.
- [7] J. R. Cloutier "Time-to-go-less guidance with cross channel couplings". In Proceedings of the AIAA Missile Sciences Conference, Monterey, CA, December 1996.
- [8] C. P. Mracek and J. R. Cloutier "Missile longitudinal autopilot design using the state-dependent Riccati equation method". In Proceedings of the International Conference on Nonlinear Problems in Aviation and Aerospace. Available through University Press, Embry-Riddle Aeronautical University, Daytona Beach, FL, 32114, May 1996.
- [9] K. A. Wise, J. L. Sedwick, and R. L. Eberhardt "Nonlinear control of missiles". McDonnell Douglas Aerospace Report MDC 93B0484, October 1993.
- [10] D. E. Williams, B. F'riedland, and A. N. Madiwale "Modern control theory for design of autopilots for bank-to-turn missiles". Journal of Guidance, Control, and Dynamics, 10(4):378-386, July-August 1987.
- [11] C. P. Mracek and J. R. Cloutier "A preliminary control design for the nonlinear benchmark problem". Proceedings of the IEEE Conference on Control Applications, Dearborn, MI, pp.265-272 DOI 10.1109/CCA.1996.558705 September 1996.
- [12] C. P. Mracek and J. R. Cloutier "Control designs for the nonlinear benchmark problem via the state dependent Riccati equation method", International Journal of Robust and Nonlinear Control Int. J. Robust Nonlinear Control 8, pp. 401-433 (1998).
- [13] J. R. Cloutier, C. N. D'Souza, and C. P. Mracek. "Nonlinear regulation and nonlinear H<sub>2</sub> control via the state-dependent Riccati equation technique"; part 1, theory; part 2, examples. Proceedings of the International Conference on Nonlinear Problems in Aviation and Aerospace. Available through University Press, Embry-Riddle Aeronautical University, Daytona Beach, FL, 32114, May 1996.
- [14] C. P. Mracek, J. R. Cloutier, and C. N. D'Souza "A new technique for nonlinear estimation". Proceedings of the IEEE Conference on Control Applications, Dearborn, MI, pp.338-343, DOI 10.1109/CCA.1996.558760 September 1996.
- [15] J. Shamma and J. Cloutier, "Existence of SDRE stabilizing controllers", IEEE Transactions on Automatic Control, pp.513-517, March 2003.
- [16] J. Willard Curtis, Randal W. Beard, "Ensuring Stability of State-Dependent Riccati Equation Controllers via Satisficing," IEEE Conference on Decision and Control, Las Vegas, NV, 2002, pp. 2645-2650, vol3.
- [17] Parkinson and Spilker, "Global position System Theory and application I, II", American Institute of Aeronautics and Astronautics, 1996, AIAA ISBN 978-1563472497
- [18] Jonghuk Kim, Salah Sukkarieh "Real-time implementation of airborne inertial-SLAM" Robotics and Autonomous Systems 55(2007)62-7, 0921-8890/ Elsevier2006.
- [19] Guoqiang Mao, Sam Drake and Brian D. O. Anderson "Design of an Extended Kalman Filter for UAV Localisation" Defence Science and Technology Organization (DSTO), Australia, DOI 10.1109/IDC.2007.374554, pp.224-229, Feb 2007.
- [20] James R.Cloutier "Navigation and Control Branch U.S. Air Force Armament Directorate", Eglin AFB, FL 32542-6810, Proceedings of the American Control Conference Albuquerque, New Mexico June 1997.
- [21] James R.Cloutier, Curtis P.Mracek, D Brett Ridgely, Kelly D.Hammett, "State-Dependent Riccati Equation Techniques: Theory and Applications" American Control Conference Workshop 1998.
- [22] David a. Haessig and Bernard Friedland "State Dependent Differential Riccati Equation for Nonlinear Estimation and Control" 15th Triennial World Congress, Barcelona, Spain. 2002 IFAC
- [23] C. C.G. Park, K. Kim, and W.Y. Kang " UKF based In-Flight Alignment using Low Cost IMU" AIAA Guidance, Navigation, and Control Conference and Exhibit, AIAA 2006-6353, Colorado, USA, 2006.
- [24] A.N. Ndjeng, D. Gruyer, A. Lambert, B. Mourllion and S. Glaser "Experimental Comparison of Bayesian. Outdoor Vehicle Localization Filters" Workshop on Safe navigation in open and dynamic environments Application to autonomous vehicles, in IEEE ICRA Conference, Kobe, Japan, 2009.